Thrombosis and Haemostasis

Volume Regulation and Non-Osmotic Volume of Individual Human Platelets Quantified by High-Speed Scanning Ion Conductance Microscopy

Konstantin Krutzke, Jan Seifert, Meinrad Gawaz, Johannes Rheinlaender, Tilman E Schäffer.

Affiliations below.

Abstract:
Platelets are anucleate cells that play an important role in wound closure following vessel injury. Maintaining a constant platelet volume is critical for platelet function. For example, water-induced swelling can promote procoagulant activity and initiate thrombosis. However, techniques for measuring changes in platelet volume such as light transmittance or impedance techniques have inherent limitations as they only allow qualitative measurements or do not work on the single-cell level. Here, we introduce high-speed scanning ion conductance microscopy (HS-SICM) as a new platform for studying volume regulation mechanisms of individual platelets. We optimized HS-SICM to quantitatively image the morphology of adherent platelets as a function of time at scanning speeds up to 7 s/frame and with 0.1 fL precision. We demonstrate that HS-SICM can quantitatively measure the rapid swelling of individual platelets after a hypotonic shock and the following regulatory volume decrease (RVD). We found that the RVD of thrombin-, ADP-, and collagen-activated platelets was significantly reduced compared to non-activated platelets. Applying the Boyle van't Hoff relationship allowed us to extract the non-osmotic volume and volume fraction on a single-platelet level. Activation by thrombin or ADP, but not by collagen, resulted in a decrease of the non-osmotic volume, likely due to a release reaction, leaving the total volume unaffected.

Corresponding Author:
Prof. Tilman E Schäffer, University of Tübingen, Institute of Applied Physics, Tubingen, Germany, tilman.schaeffer@uni-tuebingen.de

Affiliations:
Konstantin Krutzke, University of Tübingen, Institute of Applied Physics, Tubingen, Germany
Jan Seifert, University of Tübingen, Institute of Applied Physics, Tubingen, Germany
Meinrad Gawaz, University of Tübingen, Department of Internal Medicine III, Cardiology and Angiology, Tubingen, Germany
Johannes Rheinlaender, University of Tübingen, Institute of Applied Physics, Tubingen, Germany
Tilman E Schäffer, University of Tübingen, Institute of Applied Physics, Tubingen, Germany

Thieme

Volume Regulation and Non-Osmotic Volume of Individual Human Platelets Quantified by High-Speed Scanning Ion Conductance Microscopy

Konstantin Krutzke[1], Jan Seifert[1], Meinrad Gawaz[2], Johannes Rheinlaender[1], and Tilman E. Schäffer[1]

[1]Institute for Applied Physics, University of Tübingen, Tübingen, Germany
[2]Department of Internal Medicine III, Cardiology and Angiology, University of Tübingen

Correspondence to:

Tilman E. Schäffer, PhD
Institute of Applied Physics
University of Tübingen
Auf der Morgenstelle 10
72076 Tübingen, Germany
E-Mail: tilman.schaeffer@uni-tuebingen.de

Abstract

Platelets are anucleate cells that play an important role in wound closure following vessel injury. Maintaining a constant platelet volume is critical for platelet function. For example, water-induced swelling can promote procoagulant activity and initiate thrombosis. However, techniques for measuring changes in platelet volume such as light transmittance or impedance techniques have inherent limitations as they only allow qualitative measurements or do not work on the single-cell level. Here, we introduce high-speed scanning ion conductance microscopy (HS-SICM) as a new platform for studying volume regulation mechanisms of individual platelets. We optimized HS-SICM to quantitatively image the morphology of adherent platelets as

1

a function of time at scanning speeds up to 7 s/frame and with 0.1 fL precision. We demonstrate that HS-SICM can quantitatively measure the rapid swelling of individual platelets after a hypotonic shock and the following regulatory volume decrease (RVD). We found that the RVD of thrombin-, ADP-, and collagen-activated platelets was significantly reduced compared to non-activated platelets. Applying the Boyle van't Hoff relationship allowed us to extract the non-osmotic volume and volume fraction on a single-platelet level. Activation by thrombin or ADP, but not by collagen, resulted in a decrease of the non-osmotic volume, likely due to a release reaction, leaving the total volume unaffected.

Introduction

Platelets are one of the three main cellular components present in mammalian blood and play a pivotal role in human physiology, particularly in hemostasis and the intricate process of wound closure. After vessel injury, platelets are activated, adhere to extracellular matrix components such as collagen or fibrinogen, and release chemical signals to attract more platelets to the site of injury.[1,2] Platelets thereby undergo a shape change in order to close the injured vessel by agglomeration and formation of a blood clot.[3,4] Activation can be triggered by various factors,[4,5] for example, by mechanical or enzymatic stimulation,[6,7] and uncontrolled platelet activation increases the risk of thrombosis or stroke.[8,9]

Maintaining a constant platelet volume is critical for correct platelet function.[10] For example, it was shown that water-induced swelling of platelets might promote their activity and thereby initiate thrombosis.[11] Therefore, platelets have established an

2

effective volume regulation mechanism (regulatory volume decrease, RVD),[12] based on the passive transport of water by water channels (aquaporins).[11] The regulation of platelet volume is associated with a change in the osmolarity of the surrounding medium, which can be an important factor, for example, in blood transfusion.[13,14] When exposed to a rapid osmolarity change, the platelet changes its volume in response to the osmolarity change of the medium to adapt to the extracellular environment, mediated by an influx or efflux of water through aquaporins in the cell membrane into or out of the cell.[11,12,15] However, despite its potential significance, the impact of platelet activation on RVD and its role in physiological and pathological processes has not been widely investigated.[11,16] Single-cell measurements present a significant advantage in this context, as they allow for the characterization of individual platelets, thereby capturing the substantial variance that exists within platelet populations.

Methods to quantify platelet volume such as light transmittance or impedance measurements are limited as they only measure volume qualitatively or only determine the average volume of a platelet population. On the other hand, single-platelet imaging techniques such as atomic force microscopy (AFM)[6,17] or fluorescence microscopy[18,19] might induce unintended platelet activation or often require fixation or fluorescent labelling of the platelets.[17,20]

We therefore applied high-speed scanning ion conductance microscopy[21,22] (HS-SICM) to record topography image sequences of individual platelets to investigate the dynamics of water-induced swelling and subsequent volume regulation.[7,23] As HS-SICM can image live cells with submicrometer resolution without mechanical contact, it is ideal for quantitative assessment of platelet shape and volume[24] without

3

the risk of platelet activation.[7,25] For example, SICM has recently been used to study platelet morphology[26], mechanics[7], migration[25], and thrombus formation[27]. By optimizing the scanning speed and pixel resolution to measure the volume of individual platelets, we observe rapid volume changes in swelling platelets with a temporal resolution of 7 s/frame and a precision of 0.1 fL. We demonstrate that the peak volume and the swelling rate after hypotonic shock directly depend on the osmolarity of the extracellular medium. RVD was suppressed when platelets were investigated in the presence of thrombin, adenosine diphosphate (ADP), or collagen. We also showed that the non-osmotic volume in platelets was reduced in thrombin- or ADP-treated, but not in collagen-treated platelets.

Methods

Human platelet isolation and preparation

All procedures were approved by the institutional ethics committee (273/2018BO2) and comply with the declaration of Helsinki. Freshly drawn venous blood of healthy volunteers was used for platelet isolation by using monovettes filled with anti-coagulant acid citrate dextrose (at a ratio of 1:4) (04.1926.001, Sarstedt, Nümbrecht, Germany). After centrifugation at 200× g for 20 min, platelet-rich plasma (PRP) was collected and transferred into Tyrode-HEPES buffer solution (136.89 mM NaCl, 2.81 mM KCl, 11.9 mM $NaHCO_3$, 1.05 mM $MgCl_2$, 0.42 mM NaH_2PO_4, 5.56 mM D-glucose, 1 g/L BSA, 4 mM HEPES), pH 6.5, at a ratio of 1:3. After centrifugation at 880× g for 10 min, platelets were carefully resuspended in 1 mL Tyrode-HEPES buffer solution, pH 7.4. The Tyrode-HEPES buffer solution had a standard osmolarity of 295 mOsmol/L and is referred to as 'isotonic' in the following.

4

For HS-SICM measurements, washed platelets were added to a cell culture dish (627160, Greiner Bio-One GmbH, Kremsmünster, Austria). After 10 s, non-adherent platelets were removed by carefully washing three times with isotonic Tyrode-HEPES buffer solution, pH 7.4, and adherent platelets were allowed to spread for 10 min. Afterwards, the dish was mounted in the HS-SICM setup and HS-SICM measurements were carried out at room temperature.

To inhibit the RVD, washed platelets were imaged in isotonic Tyrode-HEPES buffer solution with an increased KCl (+45 mM) and a decreased NaCl (-45 mM) concentration (unchanged osmolarity; this buffer solution is referred to as high K^+ buffer and respective platelets as high K^+-treated in the following).[12]

To determine the influence of the actin cytoskeleton on the swelling and volume regulation behavior, 50 µM cytochalasin D (cytoD, Cay11330-5, Cayman Chemical Company, Michigan, USA, solved in DMSO) was added to the cell culture dish with adherent platelets during HS-SICM imaging. The solvent DMSO did not affect the platelet volume (Figure S4D).

Activation of platelets was carried out by incubating platelets in suspension for 30 s with 0.1 U/mL thrombin (T6884-250UN, Sigma-Aldrich, St. Louis, MO, USA), or 10 µM adenosine diphosphate (ADP, Sigma-Aldrich) before adhesion and spreading.[28–30] Thrombin or ADP was present at the given concentration during the whole measurement. For platelet activation with collagen[31,32], the cell culture dish was incubated with 0.1 mg/mL collagen (collagen reagens HORM, Takeda Pharma GmbH, Vienna, Austria) for 1 h at 37 °C. After incubation, the dish was washed three times with Tyrode-HEPES buffer solution, pH 7.4.

5

A commercial cell counter (impedance measurement principle, Sysmex KX-21N, Sysmex Corporation, Kobe, Japan) was used for the determination of the mean platelet volume (MPV) and the platelet distribution width (PDW) of platelets in whole blood.

HS-SICM imaging

We used a self-built HS-SICM setup with an electrolyte-filled nanopipette (Figure 1A). Nanopipettes with inner opening radii of 80-100 nm (Figure 1A, validated by scanning electron microscopy) were manufactured from borosilicate glass capillaries (Kwik-Fill glass capillaries, World Precision Instruments Inc., Florida, USA) using a CO_2-laser based pipette puller (P2000, Sutter Instruments, California, USA). The principle of HS-SICM is described elsewhere in detail.[21,25,33,34] In brief, a voltage of 250 mV, applied between two Ag/AgCl electrodes, one outside and one inside the pipette, induces an ion current that is dependent on the pipette-surface distance. The three-dimensional topography of the sample surface is acquired by using the ion current as a feedback signal and scanning the pipette over the sample using piezo actuators. The HS-SICM setup was operated in hopping/backstep mode[35] with an approach speed of 250 µm/s, an ion current trigger of 99.5% of the saturation current for the retraction of the pipette (Figure S1A, dashed lines), and a retract distance of 0.5 µm. The vertical pipette position at the trigger event was stored as the sample height at that location.

To increase the time resolution of HS-SICM imaging, we used masks for scanning only relevant regions (platelet area dilated by 2 µm and 20% random coverage of the substrate area) (Figure S1E). With 40×40 pixels per frame and a standard scan size between 15-20 µm, the typical acquisition time was 7 s/frame (Figure 1E).

6

For obtaining the MPV and the PDW using HS-SICM, the topography of adherent platelets was imaged using 100×100 μm^2 scans with a pixel resolution of 150×150 pixels.

Application of osmotic shock

To induce a hypotonic shock, the isotonic Tyrode-HEPES buffer solution (isotonic osmolarity of 295 mOsmol/L) was quickly exchanged with hypotonic buffer solution [Tyrode-HEPES buffer solution diluted with pure H_2O (HPLC quality, Fischer Chemical GmbH, Schwerte, Germany) at different volume percentages (10, 20, 30, 40, or 50% pure H_2O of the final solution)], leading to a rapid decrease in osmolarity (265, 236, 206, 177, or 147 mOsmol/L). To induce a hypertonic shock, the isotonic Tyrode-HEPES buffer solution was quickly exchanged with hypertonic buffer solution [Tyrode-HEPES buffer mixed with D-sorbitol (S1876-100G, Sigma Aldrich, Missouri, USA) at different concentrations (59, 118, or 154 mM)], leading to a rapid increase in osmolarity (354, 413, or 447 mOsmol/L) while not affecting platelet viability.[36]

For normal (untreated) platelets, platelets treated with high K^+ buffer solution, and thrombin-treated platelets, HS-SICM measurements were started 5 min before the osmotic shock was induced. For cytoD measurements, adherent platelets were treated with cytoD for 10 min before the hypotonic shock was induced (no change in cytoD concentration) and HS-SICM measurements were started 5 min before the treatment with cytoD (Figure S4C).

For solution exchange, a 3D printed (Formlabs 3, Somerville, Massachusetts, USA) cell culture dish holder with two connections, one for extracting the current buffer solution, and one for adding the exchange buffer solution, was used. HS-SICM imaging was maintained during solution exchange. Although changing the salt

concentration of the electrolyte to introduce a hypotonic shock led to a decrease in ion concentration and thus to a decrease in measured ion current (Figure S1F), the quality of HS-SICM images was almost unaffected. In the case of hypertonic shock, no decrease in image quality was observed.

HS-SICM data analysis

HS-SICM topography images of platelets were processed and analyzed using Igor Pro 9 (WaveMetrics, Inc., Portland, Oregon, USA). Platelets were identified by a pixel height threshold of $h = 50$ nm, and pixels below this threshold were considered as substrate. All topography images were corrected for tilt and z-offset by first-order line flattening.[37] To calculate the area A of each platelet, the sum of all pixel areas corresponding to the platelet was formed, $A = \sum_i a_i$. The platelet volume V was calculated by multiplying the area A with the mean height $\bar{h}$ of the platelet, $V = A \cdot \bar{h}$, which is mathematically equivalent to summing up the volumes of all pixels corresponding to the platelet (Figure 1B).[24]

For quantifying the influence of the pixel resolution on the measured platelet volume, high-resolution images (giving the 'true' volume) were downscaled with systematically varying pipette position offsets. Afterwards, the platelet volumes for the downscaled and flattened images were calculated.

The MPV was calculated as the arithmetic mean of the platelet volumes measured by HS-SICM. The PDW was measured as the width at 20% of the maximum value from log-normal distribution fits (Figures S1C, S1D).

8

For investigating the precision of the volume measurement of our HS-SICM system (Figure 1E), platelets were fixed in 2% formaldehyde for 10 min at room temperature. Then, $N = 5$ fixed platelets were imaged over time (at least 20 min).

For all time-dependent measurements, $t = 0$ was defined as the time of the hypotonic shock. The time interval before the hypotonic shock [-5 min; 0 min] was used for the calculation of the initial volume V_0 (average volume before the hypotonic shock). The relative volume was then calculated as V / V_0 with the initial volume V_0 (Figure 2C). The swelling time t_s (Figure 2C) was determined by calculating the time between the hypotonic shock (green arrow at $t = 0$) and the peak volume V_p. The platelet swelling

rate was defined as $\dfrac{V_p - V_0}{t_s}$. The regulation rate was determined as the slope of the volume between $t = 1$ and 2 min after the peak volume V_p by applying a line fit (Figure 2C). The end volume V_{end} was defined as the average volume between $t = 3$ min and 5 min after the hypotonic shock. The regulated volume was calculated as $\Delta V_{reg} = V_p - V_{end}$. Hence, for $\Delta V_{reg} \sim 0$, a platelet was interpreted as non-regulating.

The platelet-to-platelet variation of the RVD was calculated as the standard deviation σ of the relative end volume V_{end} / V_0 with standard error of the standard deviation

(SESD $= \dfrac{\sigma}{\sqrt{2 \cdot (N-1)}}$, with number of platelets N).

In order to determine the non-osmotic fraction of the platelets, we used the Boyle van't Hoff relationship[38] for cells under osmotic conditions, which assumes a linear correlation between the (relative) cell volume and the inverse tonicity[12,39] Ψ (here: ratio of the isotonic osmolarity and the hypo-/hypertonic osmolarity). For individual platelets, two data points were available: $V_0 / V_0 = 1$ at $\Psi = 1$ before the osmotic

9

shock, and V_p / V_0 at the given Ψ after the osmotic shock (before regulation). We plotted the relative platelet volumes as a function of Ψ and applied a line-fit to the data points. The value of the fit at $\Psi = 0$ gives the osmotically inactive, non-osmotic fraction of the platelets.[12] For the calculation of the non-osmotic fraction of the platelet population, the line-fit was applied to the averaged volumes at the given Ψ.

Statistical analysis

Statistical tests were carried out using Igor Pro 9 (WaveMetrics, Inc., Portland, Oregon, USA). Box plots show the median and the lower and upper quartiles. For the comparison between two groups, Student's t-test was used. For comparison between three or more groups, Tukey's range test was used. Variances were tested with the F-test for significance. The results were considered as significantly different for $P \le 0.05$ (*), $P \le 0.01$ (**), and $P \le 0.001$ (***), and as not significantly different (ns) for $P > 0.05$. Platelets from 3 to 8 independent donors were measured.

Results and Discussion

Optimization of fast volume measurements with HS-SICM

The topography of individual adherent, spread platelets was imaged using HS-SICM (Figure 1A). Platelets usually had a spread-out morphology with a flat lamellipodium at the outer regions and a higher platelet body at the center (Figure S1B). In a topography image, the platelet volume corresponds to the sum of the effective volume of all pixels of the platelet (Figure 1B). To verify that SICM accurately measures platelet volume, we compared the mean platelet volume (MPV) of three different donors as obtained from SICM topography images with the MPV measured with a conventional cell counter as "gold standard", revealing no significant

difference (Figures 1C, S1C). However, within individual donors, there was a trend for slightly larger MPV and PDW with SICM compared to the cell counter (Figure S1D). This discrepancy could likely arise from the difference in measurement conditions, since we measured adherent washed platelets with SICM as opposed to platelets from whole blood in solution with the cell counter.

The measurement speed of SICM is dependent on numerous factors and the acquisition of a topography image typically takes several minutes,[35] limiting the ability to measure rapid morphological changes of individual human platelets. The acquisition time in HS-SICM in the hopping mode is proportional to the number of pixels of the image. At a low number of pixels per image, the acquisition time is short, but the image resolution is low due to a high degree of pixelation of the platelet (Figure 1D, left image), making volume measurements less precise. To find the optimum number of pixels per platelet for a given volume precision, we recorded a high-resolution image (200×200 pixels) of a platelet and progressively down-sampled this image to generate lower-resolution images (100×100, 40×40, and 15×15 pixels) (Figure 1D, top; also see Methods). From each of these images, we measured the platelet volume (normalized by the 'true' platelet volume from the respective high-resolution image). Repeating this process for 26 images of different platelets allowed us to plot the average of the measured normalized volumes and the average precision of the volume measurements as a function of the number of pixels per platelet (Figure 1D, center and bottom). While the average normalized volume stayed constant for an increasing number of pixels per platelet (Figure 1D, center), the precision of that measurement improved (Figure 1D, bottom). For a volume measurement precision of 1% we need about $n = i$ 200 pixels per platelet (Figure 1D, bottom, red dashed line). For a typical platelet area A, this corresponds to a required

11

pixel size of $s_{px} = \sqrt{\dfrac{A}{n}}$. Assuming a circular platelet of diameter d, the required pixel

size is $s_{px} = \sqrt{\dfrac{\pi}{4n}} \cdot d = 0.063\, d$, which amounts to $d/s_{px} = 16$ pixels across the platelet.

For a typical platelet diameter of 7 µm (Figure S1B), the required pixel size is $s_{px} = 440$ nm (for 1% precision in the platelet volume measurement). In our experiments, we therefore chose an image resolution of 40×40 pixels with a scan size of 15-20 µm.

To further speed up the imaging, we reduced the number of pixels acquired on the substrate around the platelet by computing a dynamic mask around the platelet (Figure S1E, images). These optimizations facilitated a reduction in acquisition time by a factor of approximately 2.5 in this example (Figure S1E, right). As a result, we were able to capture rapid topography and volume changes of individual living platelets with acquisition times of down to 7 s/frame (Figure 1E, Figure S2A) (comparable with values reported in other HS-SICM publications[40,41]) and with a precision of typically 0.1 fL (Figure 1E, inset) (which reflects the 1% precision from the pixelation set above).

Platelet swelling after hypotonic shock

In contrast to previous studies, which measured suspended platelet volume changes in solution, averaged over a whole population of platelets, or performed only qualitative measurements,[14,15,42] our approach with HS-SICM allows capturing quantitative, time-lapse volume changes of adherent platelets undergoing hypotonic shock. Platelets showed a rapid swelling with an increase in platelet height after hypotonic shock (Figure 2A, Figure S2A, Supplementary Movie 1). Subsequently,

12

the height slowly decreased again towards almost the initial height (regulatory volume decrease, Figure 2A). From such image sequences, we measured the platelet volume V (Figure 2B, top) and the volume relative to the initial volume V_0 (Figure 2B, bottom) as a function of time. The volume of platelets exposed to a hypotonic shock of 40% H_2O rapidly increased within seconds after the shock (Figure 2B, black curves). Within ≈ 1 min after the hypotonic shock, the volume started to decrease again and became constant at ≈ 5 min. Platelets without a hypotonic shock did not show any significant increase in volume (Figure 2B, grey curves). Platelets during hypotonic shock with lower H_2O percentages generally showed a weaker volume change but a similar time behavior (Figure S2B-D). These volume dynamics can be parameterized (Figure 2C) as the initial volume V_0 before the hypotonic shock, the peak volume V_p reached at the swelling time t_s after the hypotonic shock, the end volume V_{end}, the regulated volume $\Delta V_{reg} = V_p - V_{end}$, the swelling rate, and the regulation rate.

The relative peak volume V_p / V_0 increased significantly for an increasing H_2O percentage and hence for decreasing osmolarity (Figures 2D, S2B-D). The swelling rate also increased with the H_2O percentage (Figure 2E). In contrast, the swelling time did not depend on the H_2O percentage and was therefore independent of the osmolarity (Figure S3A). This indicates that a hypotonic shock with a larger osmotic change induces a larger water influx into the platelet, which supports the assumption that the volume increase in platelets is driven by diffusion.[43,44] This assumption was further upheld by the roughly linear correlation ($r = 0.66 \pm 0.091$, $P = 3.04 \cdot 10^{-10}$) between the initial platelet volume V_0 (as a measure of platelet size) and the swelling rate (Figure S3B), showing that larger platelets with a larger surface area can take up larger amounts of H_2O per time. Consequently, the swelling rate of platelets

13

showed a significant size-dependency for a hypotonic shock with 40% H_2O when comparing small ($V_0 < 12$ fL) and large ($V_0 \geq 12$ fL) platelets (Figure S3C, left). In contrast, the regulation rate did not depend on platelet size (Figure S3C, right). For better comparison of the end volume V_{end} (volume plateau after regulation) between differently sized platelets and different H_2O percentages, we investigated the relative end volume V_{end} / V_0, showing a significant increase with H_2O percentage (Figure 2F).

The regulation rate was significantly increased ($P = 0.0012$, compared to control) only after hypotonic shock with 40% H_2O (Figure 2G). Thus, both the regulated volume ΔV_{reg} (Figure 2H) and the relative regulated volume $\Delta V_{reg} / V_0$ (Figure S3D) were significantly ($P = 0.00098$, $P = 0.00012$, respectively, compared to control) increased only after a hypotonic shock with 40% H_2O and were much smaller for 30% H_2O or lower, indicating that RVD is more pronounced at a hypotonic shock with lower osmolarity.[45] In the following, we therefore used 40% H_2O to induce a hypotonic shock. For comparison, platelets exposed to hypertonic shock rapidly shrank but did not show a notable regulatory volume increase (RVI) (Figure S2E). This aligns with previous findings that platelets, among other cell types, respond to hypertonic shrinking with activation of Na^+/H^+ exchange but do not exhibit a detectable RVI.[12] This behavior may be explained by different ion channels involved in RVD and RVI. In RVD, mainly K^+ and Cl^- are secreted[46], leading to an efficient change of the intracellular osmolarity by water efflux, whereas in RVI, mainly the Na^+/H^+ exchanger is activated, which might decrease the net gain of osmolytes in RVI[47]. However, some cell types can exhibit an effective RVI after hypertonic shock, but the reason for the different RVI behaviors is yet unknown.[48]

14

The swelling induced by the hypotonic shock primarily caused an increase in platelet height, while the platelet area did not significantly change (Figure S3E). Interestingly, for a hypotonic shock with 80% H_2O, which led to an average relative peak volume of $V_p / V_0 = 2.32$, the formation of a filopodium could be observed within minutes after the hypotonic shock (Figures S3F and G; also s. Supplementary Movies 2 and 3), which is a possible indicator of platelet apoptosis.[6] The absence of filopodia at 40% H_2O and below supports the assumption that platelet viability is not notably decreased by hypotonic shocks with lower osmolarities and that platelets can swell and regulate their volume without apoptosis.[12]

RVD of platelets is suppressed after platelet activation

To investigate the influence of platelet activation on the RVD, we first used thrombin as a potent platelet activator.[7,23] While normal (untreated) platelets showed a normal RVD after a hypotonic shock with 40% H_2O (Figure 3A, left, black traces), as already reported above, thrombin-treated platelets showed no notable RVD after the hypotonic shock, but remained at a constantly high volume (Figure 3A, left, green traces). Consequently, the regulated volume ΔV_{reg} of thrombin-treated platelets was significantly reduced ($P = 1.89 \cdot 10^{-8}$) compared to normal platelets (Figure 3B).

Taking advantage of the single-platelet resolution of HS-SICM, we calculated the platelet-to-platelet variation σ of the RVD as a function of time (Figure 3A, shaded areas) and the standard deviation σ of the relative end volume V_{end} / V_0 (Figure 3C). For thrombin-treated platelets, the platelet-to-platelet variation σ was significantly reduced ($P = 0.019$) compared to normal platelets, which indicates a more homogenous behavior of the platelets after hypotonic shock.

15

To investigate whether activation generally suppresses RVD in platelets, we further used ADP[49,50] and collagen[32] (Figure S4A) on platelets undergoing hypotonic shock (Figure 3A, center, light blue and yellow traces). Like thrombin-treated platelets, ADP and collagen both suppressed RVD after hypotonic shock with 40% H_2O as indicated by a constant high relative volume after hypotonic shock (Figure 3A). Consequently, the regulated volume ΔV_{reg} was significantly ($P = 2.75 \cdot 10^{-5}$ and $P = 7.88 \cdot 10^{-6}$, respectively) reduced compared to normal platelets (Figure 3B). Further, the platelet-to-platelet variation σ of the RVD for ADP- and collagen-treated platelets was also smaller and similar to thrombin-treated platelets (Figure 3C). Therefore, we propose that activation inhibits RVD in adherent platelets.

For comparison, we measured platelets in the presence of a high K^+ buffer, which is known to effectively inhibit the RVD.[12] As expected, platelets exposed to high K^+ buffer did not show a strong RVD (Figure 3A, right, red curves) and their regulated volume ΔV_{reg} was close to zero, significantly smaller ($P = 4.24 \cdot 10^{-10}$) than for normal platelets and similar to activated platelets (Figure 3B). Importantly, the platelet-to-platelet variation was also smaller than for normal platelets ($P = 0.00028$). During RVD, the efflux of K^+ and Cl^- ions leads to an efflux of water and a decrease in cell volume,[36,51] which is in line with the reduced efficiency of RVD in the presence of high K^+ solutions.[12,52] As the corresponding ion channels are also involved in platelet activation,[46,53] treatment with thrombin, ADP, or collagen could possibly reduce the ability of the ion channels in mediating RVD. Additionally, the absence of RVD in activated platelets may be further attributed to a change in the actin cytoskeleton and in ion channel and transporter activity.[12,54–57]

As activation is known to affect the platelet cytoskeleton, we also investigated a possible influence of the cytoskeleton on the RVD, as it is known for many cell types.[58,59] We therefore treated adherent platelets with 50 μM cytoD during HS-SICM imaging to inhibit actin polymerization (Figure S4B).[58,60] This led to a slight volume increase (Figure S4C), indicating reduced internal stress from active actin cytoskeleton remodeling during adhesion and spreading.[61–63] Despite this, the RVD was still present and the regulated volume ΔV_{reg}, the platelet-to-platelet variation σ, the initial volume V_0, and the relative peak volume V_p / V_0 after hypotonic shock with 40% H_2O were similar to normal platelets (Figure S4E-H). Therefore, RVD in platelets appears to be independent of the actin cytoskeleton, unlike for other cell types, where an intact actin cytoskeleton is crucial for effective RVD.[58,59,64]

The non-osmotic fraction of platelets varies depending on the activation agonist

The initial platelet volume V_0 was identical for all treatments (Figure 3D). The relative peak volume V_p / V_0 was significantly different for platelets treated with thrombin or ADP ($P = 0.00013$, and $P = 2.75 \cdot 10^{-5}$, respectively) (Figure 3E). In contrast, collagen-treated platelets had a similar relative peak volume V_p / V_0 as normal platelets (Figure 3E).

This observation prompted us to investigate the non-osmotic volume of platelets. Similar to other mammalian cells, the cytoplasm of platelets contains both osmotically active and inactive components[43,65] (Figure 4A). Plotting the average relative peak volume V_p / V_0 vs. the inverse tonicity (Figure 4B, top) and using the Boyle van't Hoff relationship[38] for cells under different osmotic conditions (s. Methods) allowed us to extract the non-osmotic fraction as the intercept of the

17

extrapolated line fit with the *y*-axis: 0.33 ± 0.01. This value is consistent with the literature for platelets[12] and other cells[66]. Moreover, we were able to determine the non-osmotic fraction of individual platelets (Figure 4B, bottom, intercepts with the *y*-axis). We observed a significant variation in the non-osmotic fraction among individual platelets, ranging between 0.2 and 0.5 (Figure 4C, normal) and between 1 and 12 fL (Figure 4D, normal). The non-osmotic volume was found to be proportional to the initial volume V_0 (Figure S5A). Consequently, the non-osmotic fraction was independent of the initial volume V_0 (Figure S5B).

For thrombin- or ADP-induced activation, both the non-osmotic fraction ($P = 1.4236 \cdot 10^{-5}$, $P = 2.2345 \cdot 10^{-6}$, respectively) and the non-osmotic volume ($P = 0.0319$, $P = 0.0274$, respectively) were significantly decreased by about 42% (thrombin) and 55% (ADP) compared to normal platelets (Figure 4C, D). For collagen-induced activation, in contrast, the non-osmotic fraction and volume were unchanged (Figure 4A, C, D). These observations are consistent with previous studies that have demonstrated that thrombin[67,68] and ADP[28,30] induce a "release reaction" in platelets, causing various soluble and non-soluble components, for example, granule fractions, serotonin, or platelet factor 4, to be released into the extracellular space, while collagen activation prompts the release of mostly soluble compounds[31]. Thrombin and ADP trigger the release of Ca^{2+} into the cytosol, promoting vesicle fusion with the membrane (Figure 4E, small arrows).[69,70] The extracellular release of Ca^{2+} is typically mediated by the Na^+/Ca^{2+} exchanger, which is activated as a secondary response to elevated intracellular Ca^{2+} levels.[11,53,71]

As the measured initial volume V_0 was similar for normal, thrombin- and ADP-treated platelets (Figure 3D), we hypothesize that the release of non-osmotic volume[72] into

18

the extracellular space by vesicle fusion is accompanied by an influx of water into the platelet to maintain the initial volume (Figure 4E). A possible explanation for this phenomenon could be the relief of membrane tension by exocytotic vesicle fusion, which could trigger water influx (Figure 4E, large arrow).[73]

Conclusion

We investigated dynamic volume changes of individual human platelets by topography imaging with HS-SICM. This technique permits non-invasive imaging of living cells at submicrometer spatial resolution and a time resolution on the second scale without mechanical interaction with the sample. We optimized the time resolution of HS-SICM imaging for precise volume measurement, linking a threshold of 200 pixels per platelet to a measurement precision of 1% (Figure 1D). The imaging speed was further increased by reducing the number of pixels in the background, leading to an acquisition time of 7 s/frame and a volume measurement precision of 0.1 fL (Figure 1E).

We used our HS-SICM setup to investigate the behavior of adherent and spread platelets in response to a hypotonic shock (Figure 2). The platelet volume rapidly increased after hypotonic shock and was slowly regulated back toward its initial value. The relative peak volume of platelets showed a significant volume increase with an increase in H_2O percentage, and hence a decrease in osmolarity. Moreover, the swelling rate but not the swelling time depended on the osmolarity. A pronounced RVD was observed after a hypotonic shock with 40% H_2O (Figure 2H). Contrary to some other mammalian cell types[58], RVD in platelets did not depend on the actin cytoskeleton.[74] We found that platelet activation by thrombin, ADP, or

19

collagen significantly reduced RVD of individual platelets (Figure 3), like RVD-inhibition with high K^+.

The platelet peak volume V_p followed the Boyle van't Hoff relationship for different osmotic conditions, from which we quantitatively determined the non-osmotic fraction of individual platelets as 0.33 on average (Figure 4), in good agreement with the literature. In contrast to collagen-treated platelets, thrombin- and ADP-treated platelets showed a significant decrease (42% and 55%, respectively) in the non-osmotic fraction and volume (Figure 4C, D), which has not been shown on a single-cell level before.

In conclusion, this work shows that HS-SICM is a versatile tool for resolving rapid morphological changes and volume dynamics of adherent living platelets. To further investigate and correlate vesicle fusion with our observations, future studies could utilize capacitance measurements to provide insights into potential volume changes induced by thrombin or ADP during vesicle fusion and the associated membrane surface changes.[71] Future studies could employ SICM for measuring mechanical[75] and electrical[76] properties of adherent platelets, making SICM a valuable addition to well-established technologies for measurement of suspended platelets. Such studies could provide new insights into the links between platelet volume regulation mechanisms, mechanics, membrane function, and compartmentalization in health and disease.

Acknowledgments

Author contributions

KK, JS, MG, JR, and TS designed the study. KK performed the experiments, analyzed data, and drafted the manuscript. All authors interpreted data, discussed results, and revised the manuscript.

Conflicts of interest

The authors declare no conflicts of interest.

References

1. Nurden, A. Platelets, inflammation and tissue regeneration. *Thromb Haemost* **105**, S13–S33 (2011).
2. Thomas, M. & Storey, R. The role of platelets in inflammation. *Thromb Haemost* **114**, 449–458 (2015).
3. Holinstat, M. Normal platelet function. *Cancer and Metastasis Reviews* **36**, 195–198 (2017).
4. White, J. G., Leistikow, E. L. & Escolar, G. Platelet membrane responses to surface and suspension activation. *Blood Cells* **16**, 43–72 (1990).
5. Rohlfing, A. K. *et al.* ACKR3 regulates platelet activation and ischemia-reperfusion tissue injury. *Nat Commun* **13**, 1823 (2022).
6. Posch, S. *et al.* Activation induced morphological changes and integrin αIIbβ3 activity of living platelets. *Methods* **60**, 179–185 (2013).
7. Rheinlaender, J. *et al.* Imaging the elastic modulus of human platelets during thrombininduced activation using scanning ion conductance microscopy. *Thromb Haemost* **113**, 305–311 (2015).
8. Yuri Gasparyan, A., Ayvazyan, L., P. Mikhailidis, D. & D. Kitas, G. Mean Platelet Volume: A Link Between Thrombosis and Inflammation? *Curr Pharm Des* **17**, 47–58 (2011).
9. Fitzgerald, D. J., Roy, L., Catella, F. & FitzGerald, G. A. Platelet Activation and Atherothrombosis. *New England Journal of Medicine* **315**, 983–989 (1986).
10. Colkesen, Y. & Muderrisoglu, H. The role of mean platelet volume in predicting thrombotic events. *Clin Chem Lab Med* **50**, 631–634 (2012).
11. Agbani, E. O. *et al.* Aquaporin-1 regulates platelet procoagulant membrane dynamics and in vivo thrombosis. *JCI Insight* **3**, (2018).
12. Livne, A., Grinstein, S. & Rothstein, A. Volume-regulating behavior of human platelets. *J Cell Physiol* **131**, 354–363 (1987).
13. Odink, J. Platelet Preservation. II. The Response of Human Platelet Suspensions to Hypotonic Stress. *Thromb Haemost* **36**, 182–191 (1976).

14. Kim, B. K. & Baldini, M. G. The Platelet Response to Hypotonic Shock. Its Value as an Indicator of Platelet Viability After Storage. *Transfusion (Paris)* **14**, 130–138 (1974).

15. Lee, J. S. *et al.* Water channels in platelet volume regulation. *J Cell Mol Med* **16**, 945–949 (2012).

16. Szirmai, M., Sarkadi, B., Szász, I. & Gárdos, G. Volume regulatory mechanisms of human platelets. *Haematologia (Budap)* **21**, 33–40 (1988).

17. Fritz, M., Radmacher, M. & Gaub, H. E. In Vitro Activation of Human Platelets Triggered and Probed by Atomic Force Microscopy. *Exp Cell Res* **205**, 187–190 (1993).

18. Errington, R. J. & White, N. S. Measuring dynamic cell volume in situ by confocal microscopy. *Methods Mol Biol* **122**, 315–40 (1999).

19. Klaverkamp, J. & Volkl, K. P. Maintenance of Platelet Viability after Platelet-Labeling with Fluorescein Isothiocyanate. *Pathophysiol Haemost Thromb* **14**, 337–346 (1984).

20. Nakamura, T. *et al.* Effect of low concentration of epinephrine on human platelet aggregation analyzed by particle counting method and confocal microscopy. *Journal of Laboratory and Clinical Medicine* **130**, 262–270 (1997).

21. Hansma, P. K., Drake, B., Marti, O., Gould, S. A. C. & Prater, C. B. The scanning ion-conductance microscope. *Science* **243**, 641–643 (1989).

22. Korchev, Y. E., Bashford, C. L., Milovanovic, M., Vodyanoy, I. & Lab, M. J. Scanning ion conductance microscopy of living cells. *Biophys J* **73**, 653–658 (1997).

23. Seifert, J., Rheinlaender, J., Lang, F., Gawaz, M. & Schäffer, T. E. Thrombin-induced cytoskeleton dynamics in spread human platelets observed with fast scanning ion conductance microscopy. *Sci Rep* **7**, 4810 (2017).

24. Korchev, Y. E. *et al.* Cell volume measurement using scanning ion conductance microscopy. *Biophys J* **78**, 451 (2000).

25. Seifert, J., Rheinlaender, J., von Eysmondt, H. & Schäffer, T. E. Mechanics of migrating platelets investigated with scanning ion conductance microscopy. *Nanoscale* **14**, 8192–8199 (2022).

26. Liu, X. *et al.* Use of non-contact hopping probe ion conductance microscopy to investigate dynamic morphology of live platelets. *Platelets* **26**, 480–485 (2015).

27. Nestele, J. A. *et al.* Characterization of GPVI- or GPVI-CD39-Coated Nanoparticles and Their Impact on In Vitro Thrombus Formation. *Int J Mol Sci* **23**, 11 (2021).

28. Puri, R. N., Colman, R. W. & Liberman, M. A. ADP-lnduced Platelet Activation. *Crit Rev Biochem Mol Biol* **32**, 437–502 (1997).

29. Gawaz, M., Geisler, T. & Borst, O. Current concepts and novel targets for antiplatelet therapy. *Nat Rev Cardiol* **20**, 583–599 (2023).

30. Daniel, J. L. *et al.* Molecular Basis for ADP-induced Platelet Activation. *Journal of Biological Chemistry* **273**, 2024–2029 (1998).

31. Ollivier, V. *et al.* Collagen Can Selectively Trigger a Platelet Secretory Phenotype via Glycoprotein VI. *PLoS One* **9**, e104712 (2014).

32. Roberts, D. E., McNicol, A. & Bose, R. Mechanism of Collagen Activation in Human Platelets. *Journal of Biological Chemistry* **279**, 19421–19430 (2004).

33. Shibata, M., Watanabe, H., Uchihashi, T., Ando, T. & Yasuda, R. High-speed atomic force microscopy imaging of live mammalian cells. *Biophys Physicobiol* **14**, 127–135 (2017).

34. Rheinlaender, J., Geisse, N. A., Proksch, R. & Schäffer, T. E. Comparison of scanning ion conductance microscopy with atomic force microscopy for cell imaging. *Langmuir* **27**, 697–704 (2011).

35. Novak, P. *et al.* Nanoscale live-cell imaging using hopping probe ion conductance microscopy. *Nat Methods* **6**, 279–281 (2009).

36. Lang, F. Mechanisms and Significance of Cell Volume Regulation. *J Am Coll Nutr* **26**, 613S-623S (2007).

37. Rheinlaender, J. & Schäffer, T. E. Lateral Resolution and Image Formation in Scanning Ion Conductance Microscopy. *Anal Chem* **87**, 7117–7124 (2015).

38. Nobel, P. S. The Boyle-Van't Hoff relation. *J Theor Biol* **23**, 375–379 (1969).

39. Zhou, E. H. *et al.* Universal behavior of the osmotically compressed cell and its analogy to the colloidal glass transition. *Proceedings of the National Academy of Sciences* **106**, 10632–10637 (2009).

40. Simeonov, S. & Schäffer, T. E. High-speed scanning ion conductance microscopy for sub-second topography imaging of live cells. *Nanoscale* **11**, 8579–8587 (2019).

41. Watanabe, S., Kitazawa, S., Sun, L., Kodera, N. & Ando, T. Development of high-speed ion conductance microscopy. *Review of Scientific Instruments* **90**, (2019).

42. Summerer, M. H., Genco, P. V. & Katz, A. J. The response of human platelets to hypotonic stress: direct measurement of volume change. *Ann Clin Lab Sci* **8**, 447–452 (1978).

43. Meyer, M. M. & Verkman, A. S. Human platelet osmotic water and nonelectrolyte transport. *American Journal of Physiology-Cell Physiology* **251**, C549–C557 (1986).

44. Wong, K. R. & Verkman, A. S. Human platelet diffusional water permeability measured by nuclear magnetic resonance. *American Journal of Physiology-Cell Physiology* **252**, C618–C622 (1987).

45. Watanabe, E. & Sasakawa, S. Changes of platelet cell volumes in hypotonic solution. *Thromb Res* **31**, 13–21 (1983).

46. Wright, J. R. & Mahaut-Smith, M. P. Why do platelets express K+ channels? *Platelets* **32**, 872–879 (2021).

47. Hoffmann, E. K. & Dunham, P. B. Membrane Mechanisms and Intracellular Signalling in Cell Volume Regulation. in 173–262 (1995). doi:10.1016/S0074-7696(08)62498-5.

48. O'Neill, W. C. Physiological significance of volume-regulatory transporters. *American Journal of Physiology-Cell Physiology* **276**, C995–C1011 (1999).

49. Beck, F. *et al.* Temporal quantitative phosphoproteomics of ADP stimulation reveals novel central nodes in platelet activation and inhibition. *Blood* **129**, e1–e12 (2017).

50. Trumel, C. *et al.* A Key Role of Adenosine Diphosphate in the Irreversible Platelet Aggregation Induced by the PAR1-Activating Peptide Through the Late Activation of Phosphoinositide 3-Kinase. *Blood* **94**, 4156–4165 (1999).

51. Margalit, A. & Livne, A. A. Lipoxygenase Product Controls the Regulatory Volume Decrease of Human Platelets. *Platelets* **2**, 207–214 (1991).

52. von Kügelgen, I. & Hoffmann, K. Pharmacology and structure of P2Y receptors. *Neuropharmacology* **104**, 50–61 (2016).

23

53. de Silva, H. A., Carver, J. G. & Aronson, J. K. Pharmacological Evidence of Calcium-Activated and Voltage-Gated Potassium Channels in Human Platelets. *Clin Sci* **93**, 249–255 (1997).

54. Jennings, L. K., Fox, J. E., Edwards, H. H. & Phillips, D. R. Changes in the cytoskeletal structure of human platelets following thrombin activation. *Journal of Biological Chemistry* **256**, 6927–6932 (1981).

55. Rosskopf, D. Sodium-hydrogen exchange and platelet function. *J Thromb Thrombolysis* **8**, 15–24 (1999).

56. Díaz-Ricart, M. *et al.* Inhibition of Cytoskeletal Assembly by Cytochalasin B Prevents Signaling Through Tyrosine Phosphorylation and Secretion Triggered by Collagen but Not by Thrombin. *Am J Pathol* **160**, 329–337 (2002).

57. May, J. A., Glenn, J. R., Spangenberg, P. & Heptinstall, S. The composition of the platelet cytoskeleton following activation by ADP: effects of various agents that modulate platelet function. *Platelets* **7**, 159–168 (1996).

58. Blase, C., Becker, D., Kappel, S. & Bereiter-Hahn, J. Microfilament dynamics during HaCaT cell volume regulation. *Eur J Cell Biol* **88**, 131–139 (2009).

59. Galizia, L. *et al.* Functional interaction between AQP2 and TRPV4 in renal cells. *J Cell Biochem* **113**, 580–589 (2012).

60. Casella, J., Flanagan, M. & Lin, S. Cytochalasin D inhibits actin polymerization and induces depolymerization of actin filaments formed during platelet shape change. *Nature* **293**, 300–302 (1981).

61. Beussman, K. M. *et al.* Black dots: High-yield traction force microscopy reveals structural factors contributing to platelet forces. *Acta Biomater* **163**, 302–311 (2023).

62. Paknikar, A. K., Eltzner, B. & Köster, S. Direct characterization of cytoskeletal reorganization during blood platelet spreading. *Prog Biophys Mol Biol* **144**, 166–176 (2019).

63. Zaninetti, C., Sachs, L. & Palankar, R. Role of Platelet Cytoskeleton in Platelet Biomechanics: Current and Emerging Methodologies and Their Potential Relevance for the Investigation of Inherited Platelet Disorders. *Hamostaseologie* **40**, 337–347 (2020).

64. Downey, G. P., Grinstein, S., Sue-A-Quan, A., Czaban, B. & Chan, C. K. Volume regulation in leukocytes: Requirement for an intact cytoskeleton. *J Cell Physiol* **163**, 96–104 (1995).

65. Peckys, D. B., Kleinhans, F. W. & Mazur, P. Rectification of the Water Permeability in COS-7 Cells at 22, 10 and 0°C. *PLoS One* **6**, e23643 (2011).

66. Armitage, W. J. & Juss, B. K. Osmotic response of mammalian cells: Effects of permeating cryoprotectants on nonsolvent volume. *J Cell Physiol* **168**, 532–538 (1996).

67. Hagen, I. Effects of thrombin on washed, human platelets: Chnages in the subcellular fractions. *Biochimica et Biophysica Acta (BBA) - General Subjects* **392**, 242–254 (1975).

68. Baenziger, N. L., Brodie, G. N. & Majerus, P. W. Isolation and Properties of a Thrombin-sensitive Protein of Human Platelets. *Journal of Biological Chemistry* **247**, 2723–2731 (1972).

69. Siffert, W., Siffert, G., Scheid, P. & Akkerman, J. W. Activation of Na+/H+ exchange and Ca2+ mobilization start simultaneously in thrombin-stimulated platelets. Evidence that platelet shape change disturbs early rises of BCECF fluorescence which causes an underestimation of actual cytosolic alkalinization. *Biochem J* **258**, 521–7 (1989).

70. Reed, G. L., Fitzgerald, M. L. & Polgár, J. Molecular mechanisms of platelet exocytosis: insights into the 'secrete' life of thrombocytes. *Blood* **96**, 3334–42 (2000).

71. Fernandez, J. M., Neher, E. & Gomperts, B. D. Capacitance measurements reveal stepwise fusion events in degranulating mast cells. *Nature* **312**, 453–455 (1984).

72. Hsu-Lin, S., Berman, C. L., Furie, B. C., August, D. & Furie, B. A platelet membrane protein expressed during platelet activation and secretion. Studies using a monoclonal antibody specific for thrombin-activated platelets. *Journal of Biological Chemistry* **259**, 9121–9126 (1984).

73. Apodaca, G. Modulation of membrane traffic by mechanical stimuli. *American Journal of Physiology-Renal Physiology* **282**, F179–F190 (2002).

74. Henson, J. H. Relationships between the actin cytoskeleton and cell volume regulation. *Microsc Res Tech* **47**, 155–162 (1999).

75. Schäffer, T. E. Nanomechanics of Molecules and Living Cells with Scanning Ion Conductance Microscopy. *Anal Chem* **85**, 6988–6994 (2013).

76. Chen, C.-C., Zhou, Y. & Baker, L. A. Scanning Ion Conductance Microscopy. *Annual Review of Analytical Chemistry* **5**, 207–228 (2012).
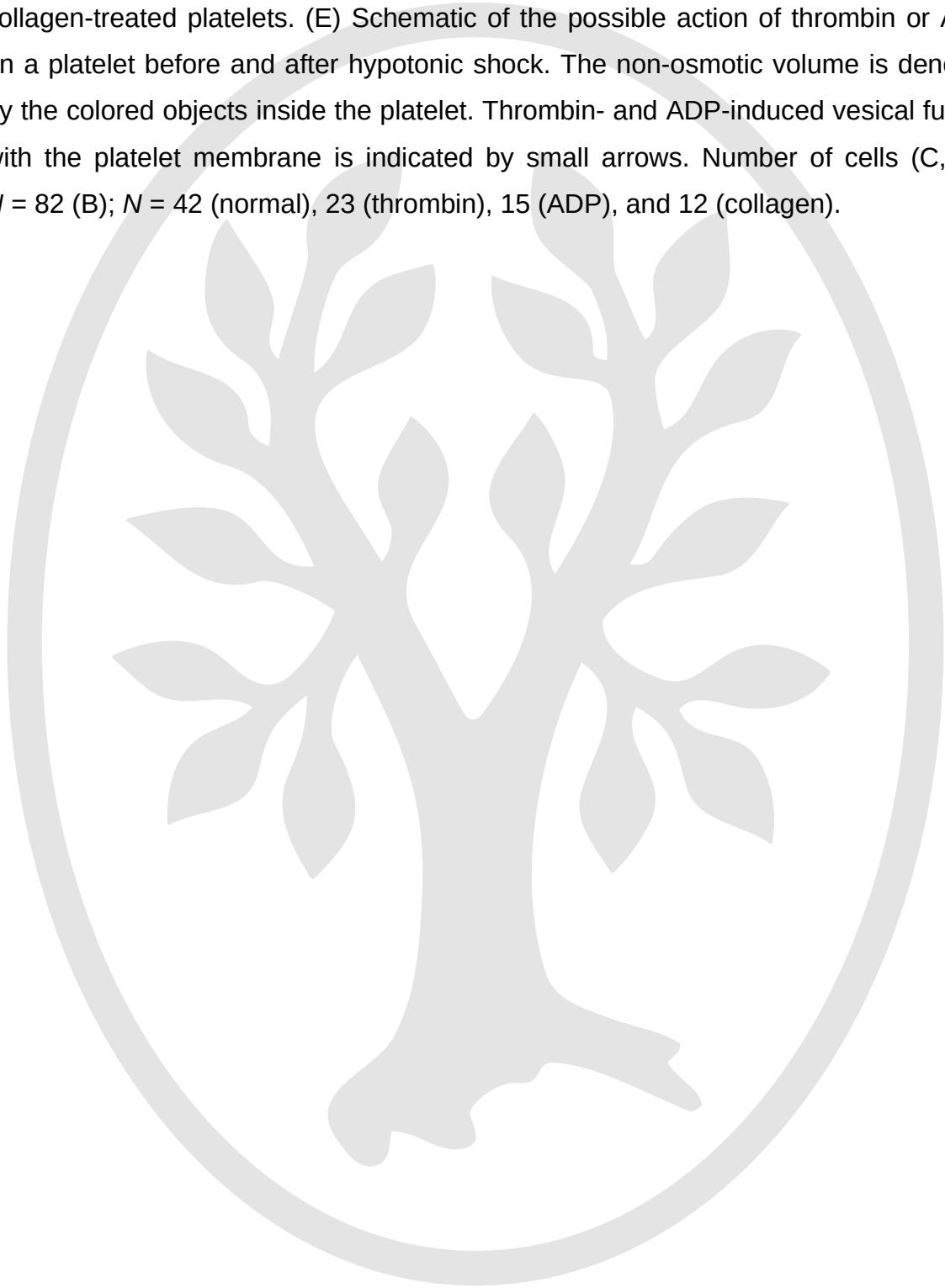
Figure 1: Platelet topography imaging and volume measurement with HS-SICM. (A) Schematic of the HS-SICM setup using a nanopipette (inset shows scanning electron microscopy image, pipette inner opening radius 90 nm) that is moved relative to the sample in the *x*-, *y*- and *z*-directions by piezo scanners. A bias voltage U_0 applied between two electrodes induces a distance-dependent ion current I_0 (also see Figure S1A). The sample buffer solution can be exchanged by using an inlet and an outlet to induce an osmotic shock. (B) Schematic for the calculation of platelet volume from the pixels of a topography image. (C) Average MPV of platelets measured with HS-SICM and a cell counter. (D) HS-SICM topography images (top row) with different pixel resolutions (15×15, 40×40, and 100×100 pixels, resulting in 24, 184, and 1146 pixels per platelet). Normalized volume (middle row) and volume measurement precision (bottom row) averaged over down-sampled platelet images for $N = 26$ platelets vs. number of pixels per platelet. A volume measurement precision of 1% (red dashed line) corresponds to about 200 pixels per platelet. Error bars show the standard deviation for normalized volume (middle row) and SESD for measurement precision (bottom row). (E) Volume measured for one fixed platelet over time with HS-SICM at 7 s/frame. The histogram (inset) shows the volume distribution giving 0.1 fL precision (standard deviation).

Figure 2: Quantitative single-platelet volume measurements with HS-SICM, resolving rapid volume dynamics of living platelets after hypotonic shock. (A) Sequence of topography images (top) and corresponding height profiles (bottom). The dashed line corresponds to the platelet before exposure to a hypotonic shock of 40% H_2O at $t = 0$ s. Every 3rd image is shown. The complete image sequence is shown in Supplementary Figure S2A and in Supplementary Movie 1. The hypotonic shock induces a rapid height increase (swelling) of the platelet, followed by a slower height decrease (regulatory volume decrease). (B) Time dynamics of the volume (top) and the volume relative to the initial volume V_0 (bottom) of individual platelets exposed to a hypotonic shock at $t = 0$ with 40% H_2O (black curves) or 0% H_2O (gray curves, control). (C) Representative volume-vs-time curve showing the definitions of the initial volume V_0, the peak volume (V_p), the regulated volume (ΔV_{reg}), the final volume (V_{end}), the swelling time t_s, the swelling rate, and the regulation rate. (D) Relative peak volume V_p / V_0 after a hypotonic shock with varying osmolarity. (E) Swelling rate, (F) relative end volume V_{end} / V_0, and (G) regulation rate for a hypotonic shock with varying osmolarity. (H) Regulated volume ΔV_{reg} of platelets after a hypotonic shock with varying osmolarity. Number of platelets (D-H): $N = 12$ (0% H_2O), 10 (10%), 11 (10%), 9 (30%), 42 (40%).
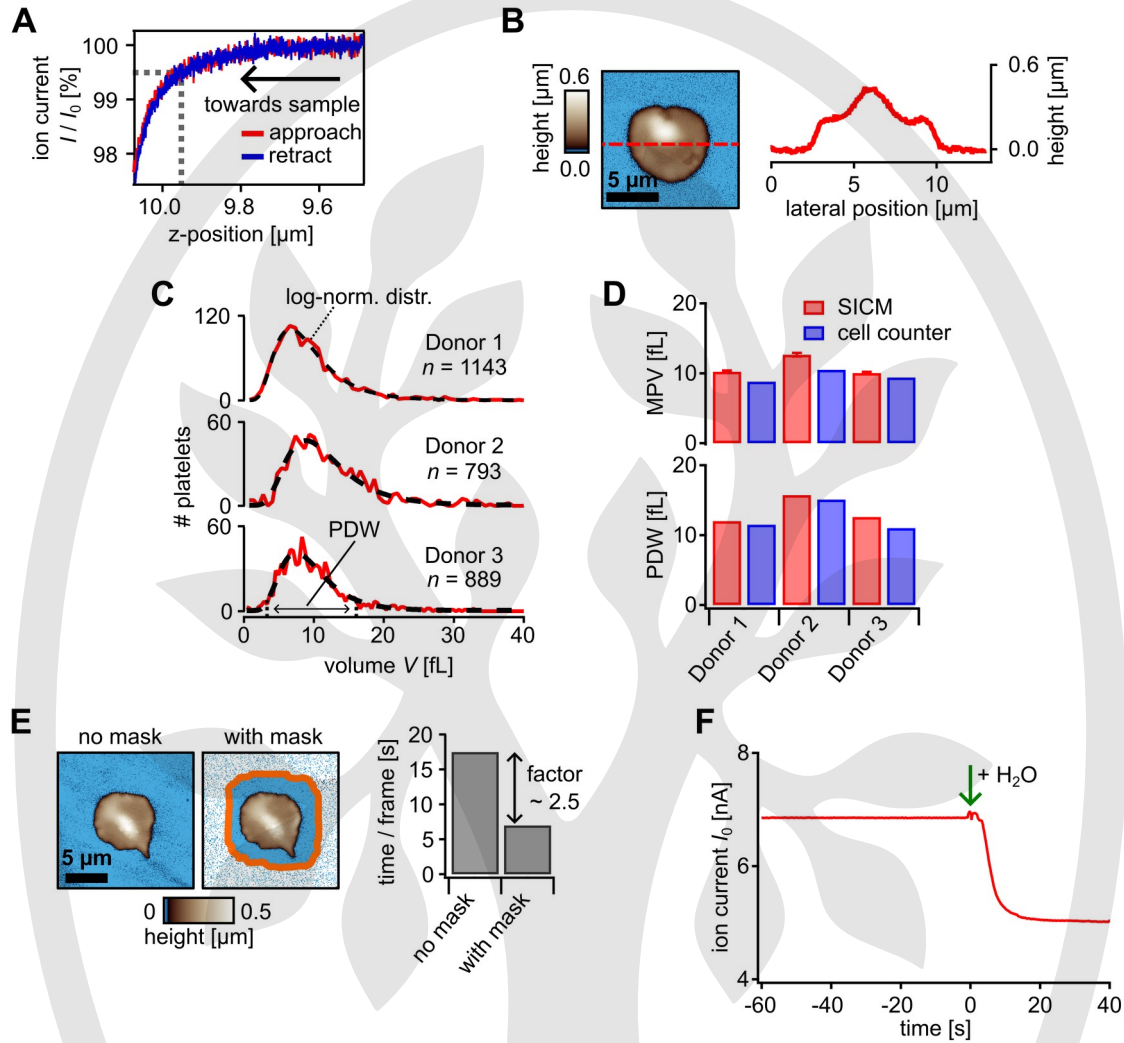
Figure 3: RVD of individual platelets after a hypotonic shock with 40% H_2O. (A) Relative volume-vs-time of representative individual platelets (dashed lines) during a hypotonic shock for different platelet treatments. Solid lines and shaded areas represent the mean and standard deviation, respectively, of all measured platelets. (B) Regulated volume ΔV_{reg} for normal (untreated), thrombin-treated, ADP-treated, collagen-treated, and high K^+-treated platelets. (C) Variation σ of the relative end volume V_{end} / V_0. Error bars show the SESD. (D) Initial volume V_0 and (E) relative peak volume V_p / V_0 for different platelet treatments. Significance in (C) was determined using the F-test. Number of cells (B-E): $N = 43$ (normal), 23 (thrombin), 15 (ADP), 12 (collagen), 28 (high K^+).

Figure 4: Determination of the non-osmotic fraction of swelling platelets with HS-SICM. (A) Schematic of the behavior of the non-osmotic fraction during hypotonic shock of normal or collagen-treated platelets. (B) Relative peak volume V_p / V_0 vs. the inverse tonicity Ψ averaged for many normal platelets (top) and for three individual

26

normal platelets (bottom). Following the Boyle van't Hoff relationship, the osmotically inactive, non-osmotic volume fraction is given by the y-intercept of the line. (C) Non-osmotic fraction and (D) non-osmotic volume of normal, thrombin-, ADP-, and collagen-treated platelets. (E) Schematic of the possible action of thrombin or ADP on a platelet before and after hypotonic shock. The non-osmotic volume is denoted by the colored objects inside the platelet. Thrombin- and ADP-induced vesical fusion with the platelet membrane is indicated by small arrows. Number of cells (C, D): $N = 82$ (B); $N = 42$ (normal), 23 (thrombin), 15 (ADP), and 12 (collagen).

A

ion current I/I_0 [%]

towards sample
approach
retract

z-position [μm]

B

height [μm]

5 μm

lateral position [μm]

height [μm]

C

log-norm. distr.

Donor 1
$n = 1143$

platelets

Donor 2
$n = 793$

PDW

Donor 3
$n = 889$

volume V [fL]

D

SICM
cell counter

MPV [fL]

PDW [fL]

Donor 1   Donor 2   Donor 3

E

no mask   with mask

5 μm

height [μm]

time / frame [s]

factor
~ 2.5

no mask   with mask

F

ion current I_0 [nA]

+ H_2O

time [s]

Figure S1: (A) Ion current as a function of the *z*-position. The current decreases with a decreasing pipette-sample distance. The dashed lines indicate the current drop at 99.5% of the saturation current I_0 with the corresponding *z*-position. (B) High-resolution topography image of a platelet and its height profile along the dashed line. (C) HS-SICM platelet volume distributions for 3 individual donors and log-normal fit (black dashed curves). (D) Comparison of MPV and PDW measurements using HS-SICM and a cell counter (gold standard). The MPV and the PDW calculated from the HS-SICM data on washed platelets are in good agreement (within 10-25% deviation) with the values from the cell counter (data acquired from whole blood). (E) Imaging speed improvement (factor 2.5) by reducing the number of pixels on the substrate. (F) Saturation ion current I_0 as a function of time before and after the exchange of the isotonic buffer solution with a hypotonic buffer solution with 40% H_2O at $t = 0$ s.
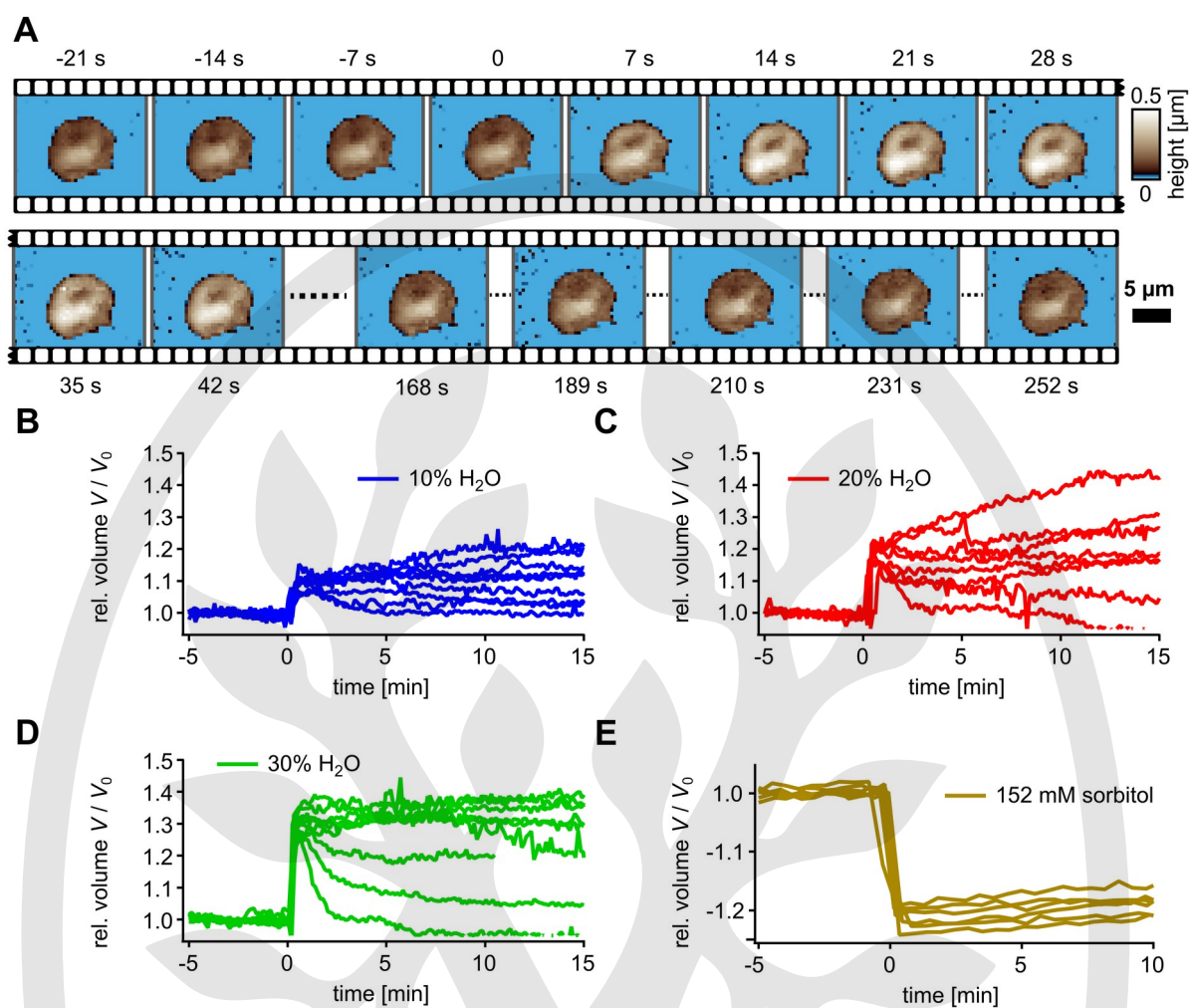
Figure S2: (A) Platelet topography image series of Figure 1C showing more frames at the used frame rate of 7 s/frame. A hypotonic shock with 40% H_2O was induced at time t = 0. (B-E) Volume-vs-time curves of individual platelets at different osmotic shock conditions (B: 10% H_2O; C: 20% H_2O; D: 30% H_2O; E: 152 mM sorbitol).
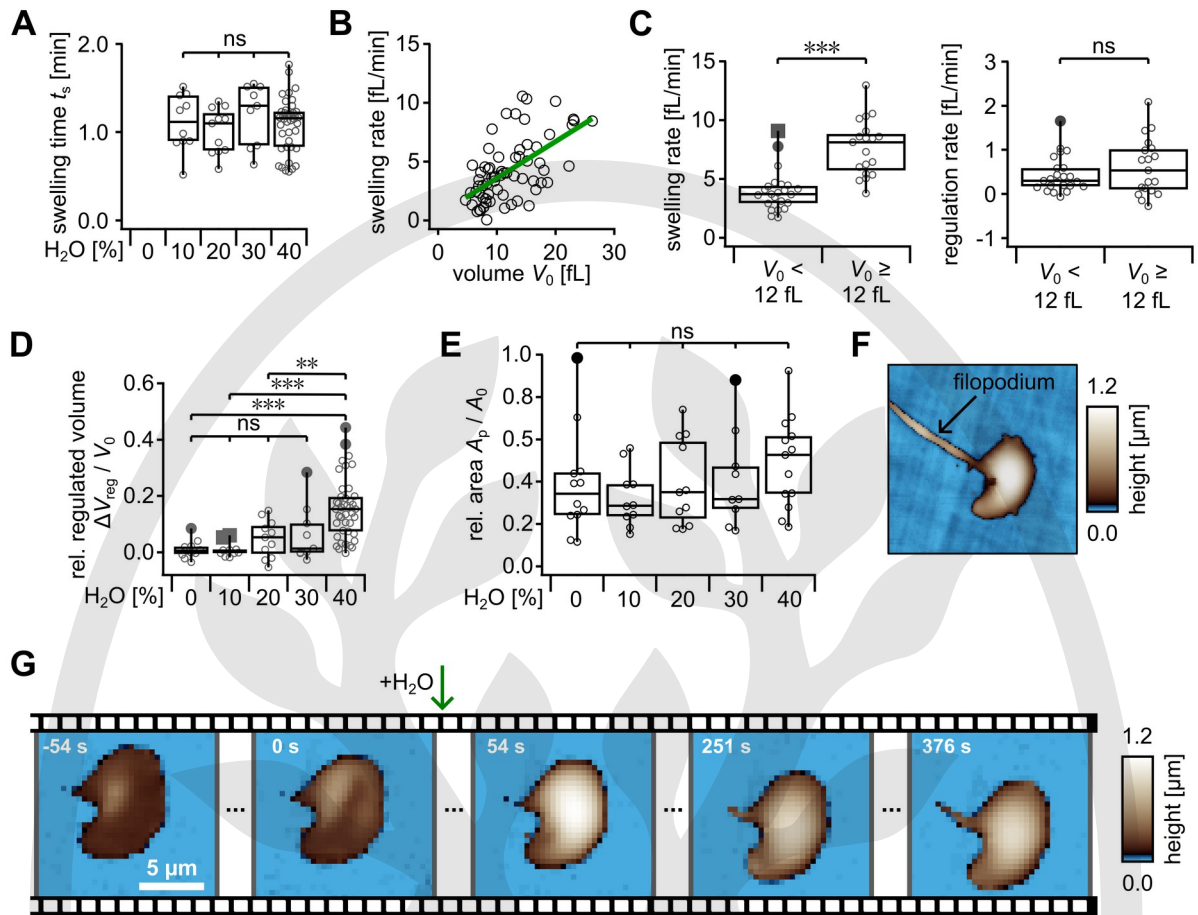
Figure S3: (A) Swelling time t_s for a hypotonic shock with different osmolarities. (B) Swelling rate as a function of the initial volume V_0, showing a linear correlation. (C) Swelling rate (left) and regulation rate (right) of small ($V_0 < 12$ fL) and large ($V_0 \geq 12$ fL) platelets, at a hypotonic shock with 40% H_2O. (D) Relative regulated volume $\Delta V_{reg} / V_0$ for different H_2O percentages. (E) Relative area (A_p / A_0) at $t = t_s$ for different H_2O percentages, with initial area A_0. (F) Platelet topography image after hypotonic shock with 80% H_2O showing the formation of a filopodium (arrow). (G) Topography image series of a platelet showing filopodia formation ($t = 376$ s), see Supplementary Movie 3 for the complete image sequence. A hypotonic shock with 80% H_2O was induced at time $t = 0$.
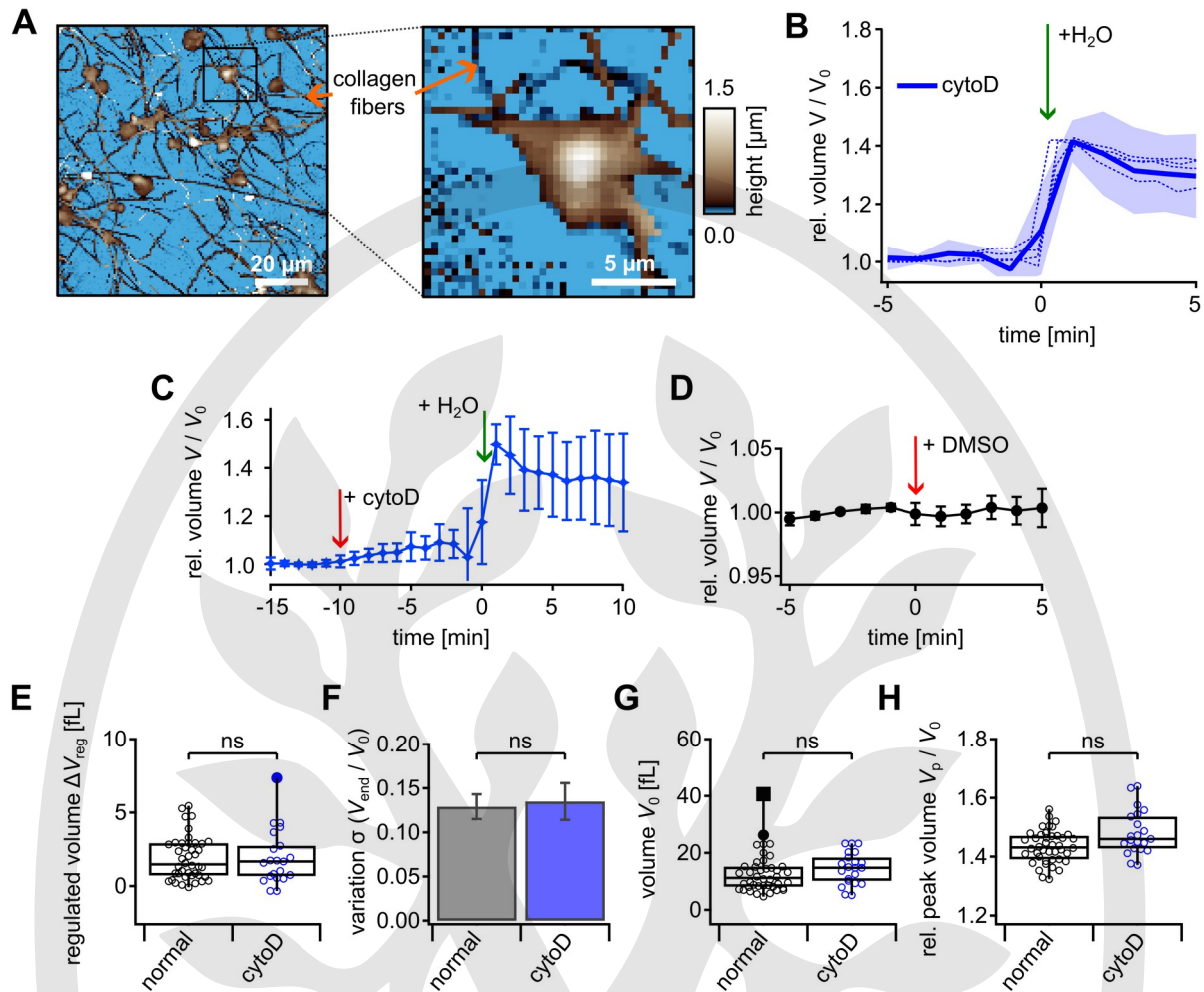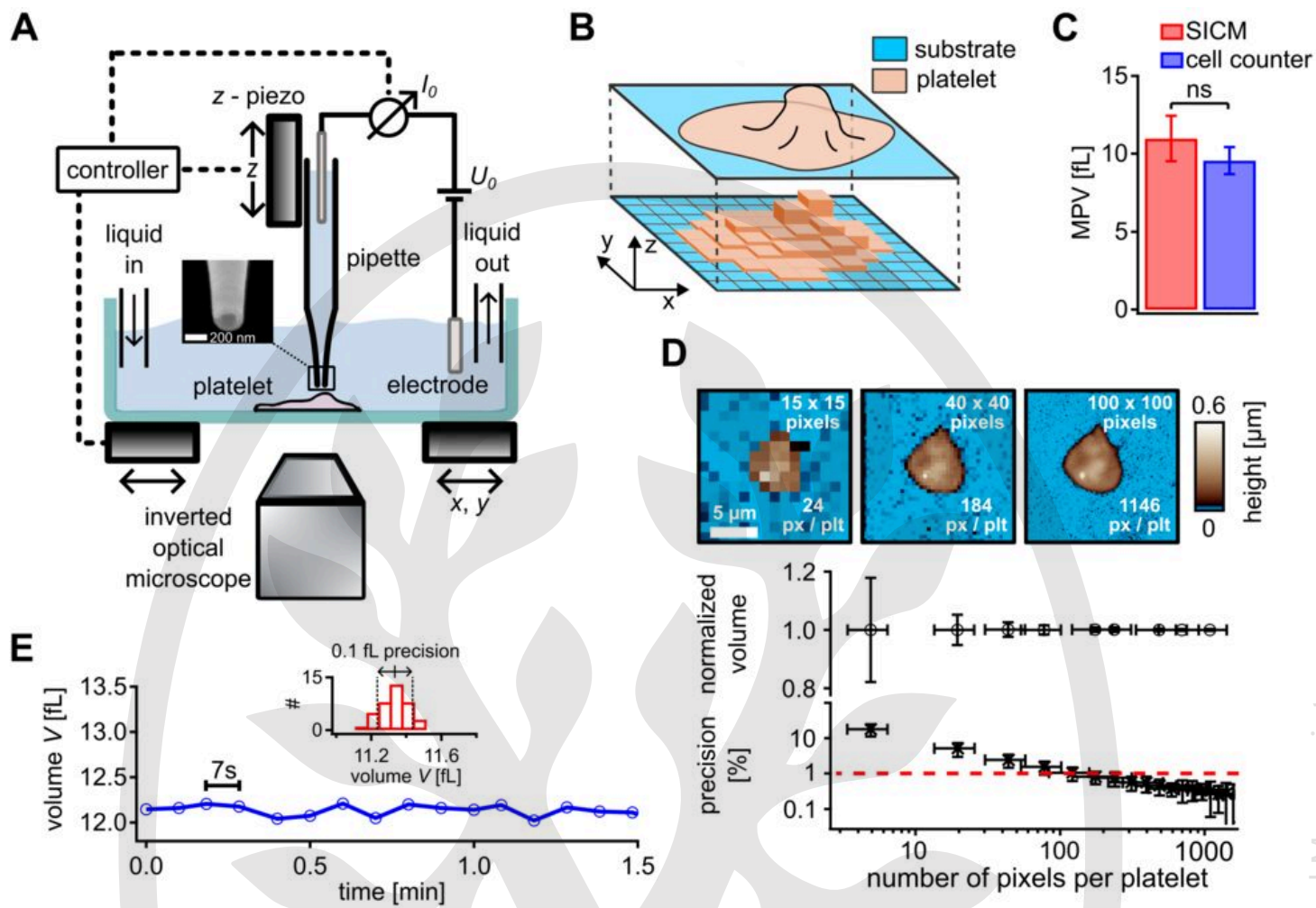
Figure S4: (A) Representative SICM topography overview image of platelets on collagen fibers (left) with a zoom-in to a single platelet (right). (B) Relative volume-vs-time of representative individual platelets (dashed lines) during a hypotonic shock for cytoD-treated platelets. Solid lines and shaded areas represent the mean and standard deviation, respectively, of all measured cytoD-treated platelets. (C) Average relative platelet volume (V / V_0) vs. time during addition of cytoD at t = -10 min and hypotonic shock with 40% H_2O at t = 0 (N = 21). (D) Average relative platelet volume (V / V_0) vs. time during addition of DMSO at t = 0 min (N = 19), as a control for the cytoD measurements. Error bars denote standard deviation. (E) Regulated volume ΔV_{reg} for normal (untreated) and cytoD-treated platelets. (F) Variation σ of the relative end volume V_{end} / V_0 for normal and cytoD-treated platelets. Error bars denote the SESD. (G) Initial volume V_0 and (H) relative peak volume V_p / V_0. Significance in (F) was determined using the F-test.
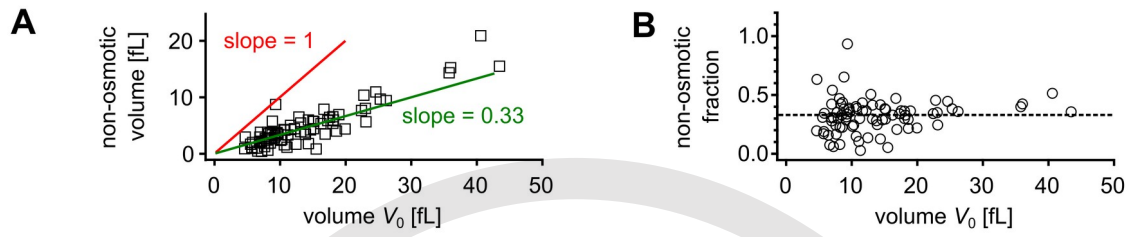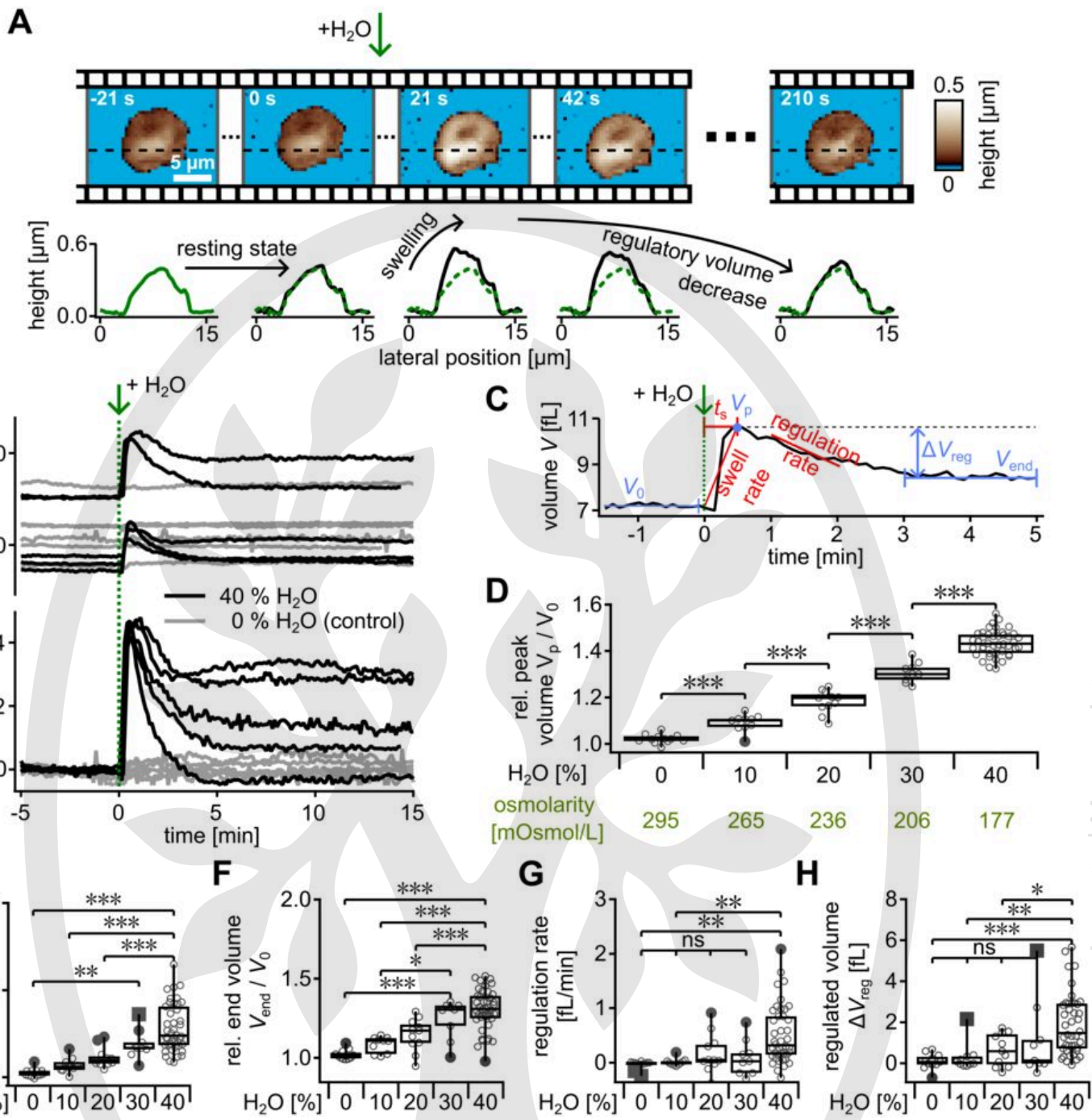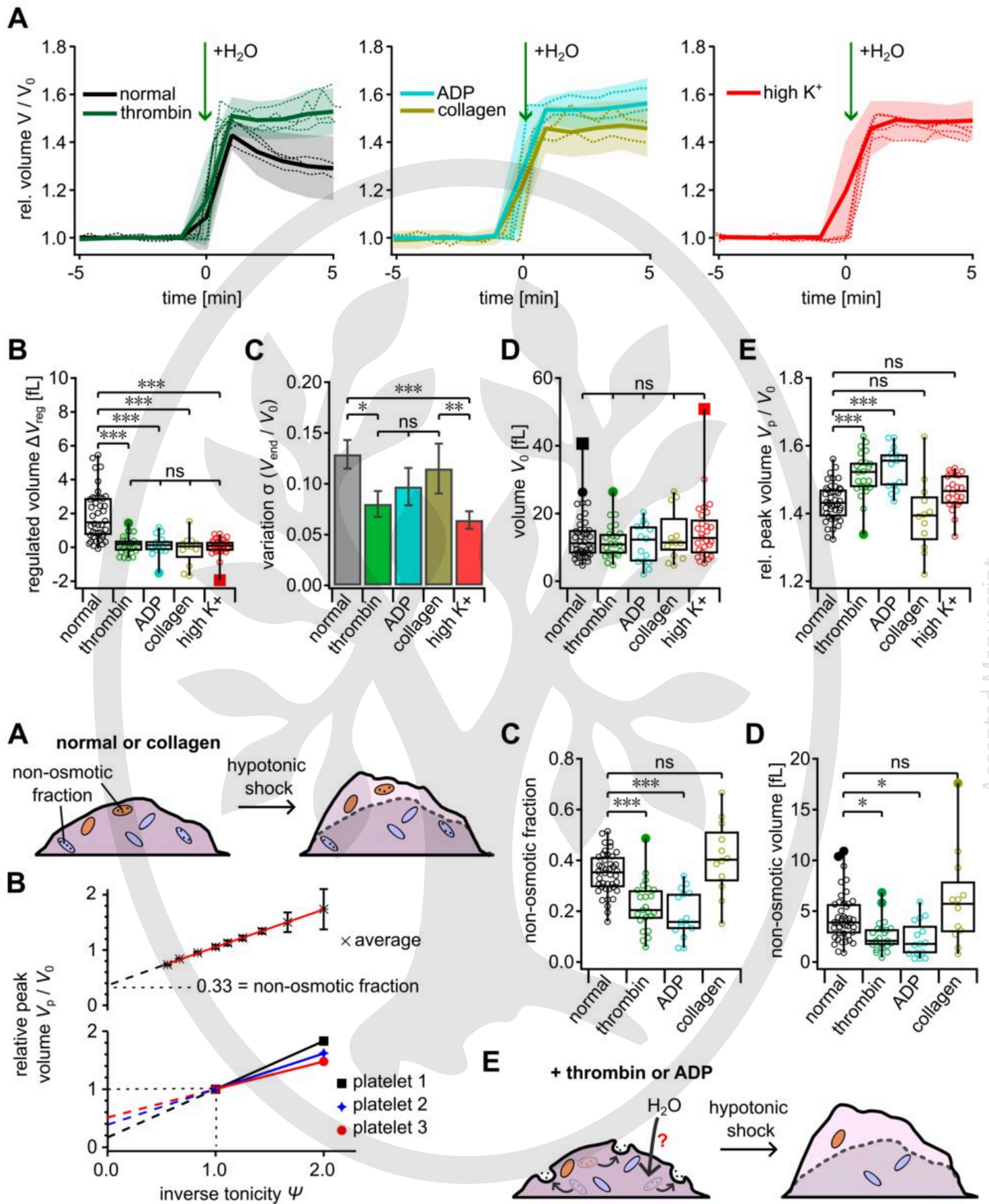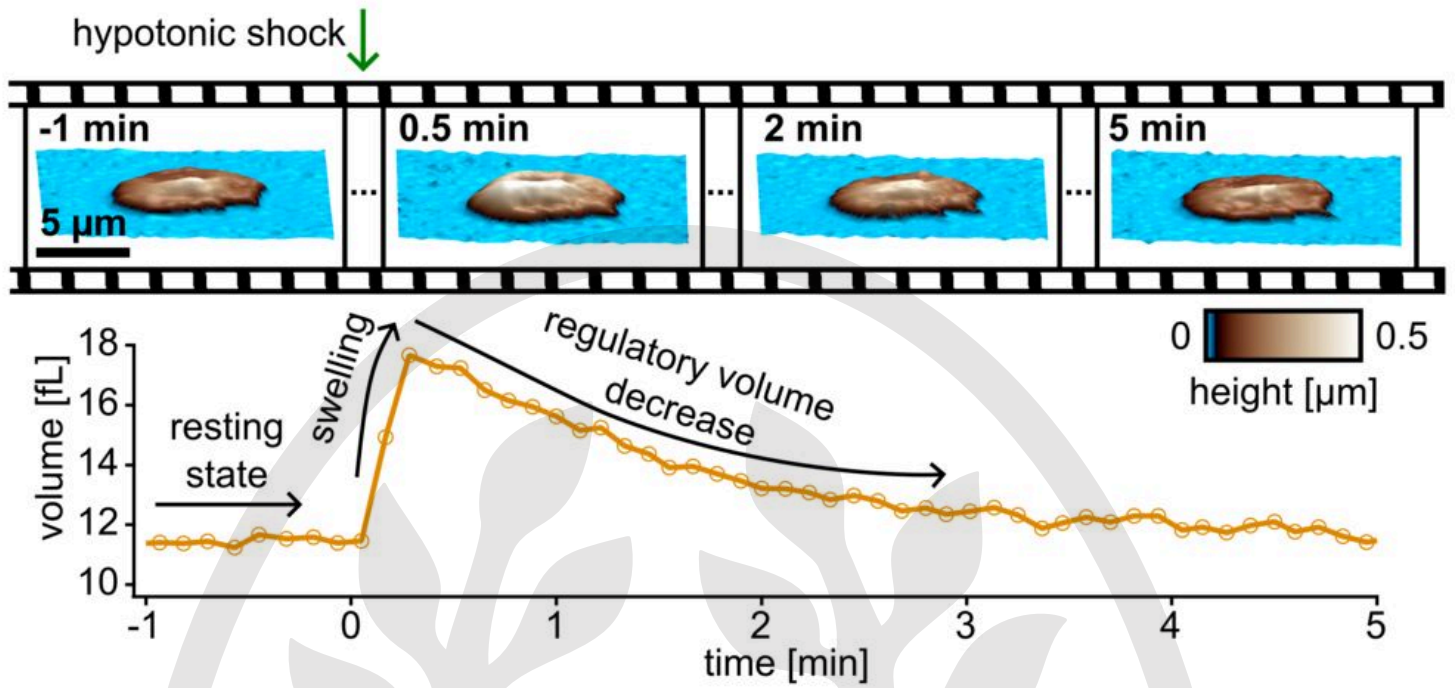
Figure S5: (A) Non-osmotic volume (green slope corresponds to a non-osmotic fraction of 0.33 ± 0.01 that is independent of V_0) and (B) non-osmotic fraction vs. the initial volume V_0 for all measured normal platelets.

What is known about this topic?	• Platelets show a regulatory volume decrease after hypotonic shock • Measurements of platelet volume regulation have been performed qualitatively on large platelet ensembles
What does this paper add?	• Quantitative, time-resolved measurement of the volume regulation after hypotonic shock of individual platelets using HS-SICM • The regulatory volume decrease is suppressed in activated platelets • Determination of the non-osmotic fraction of individual platelets via the Boyle van't Hoff relationship • Thrombin- and ADP-activated platelets show a decreased non-osmotic fraction

A

z - piezo

I_0

controller

z

U_0

liquid in

liquid out

200 nm

pipette

platelet

electrode

inverted optical microscope

x, y

B

■ substrate
■ platelet

y z

x

C

■ SICM
■ cell counter

ns

MPV [fL]

15

10

5

0

D

15 x 15 pixels

40 x 40 pixels

100 x 100 pixels

0.6

height [μm]

0

5 μm

24 px / plt

184 px / plt

1146 px / plt

normalized volume

1.2

1.0

0.8

precision [%]

10

1

0.1

number of pixels per platelet

10   100   1000

E

0.1 fL precision

#

15

11.2   11.6
volume *V* [fL]

volume *V* [fL]

13.5

13.0

12.5

12.0

7s

0.0   0.5   1.0   1.5
time [min]

Visual summary. Measuring platelet volume under hypotonic shock with high-speed SICM quantitatively resolves platelet swelling and regulation at the single-cell level.